Numerical Evaluation of Circuit Model for Fast Computational Analysis of Resonant Wireless Power Transfer System

F. Freitas, I. Soares, L. Krahenbuhl, Arnaud Bréard, C. Vollaire, S. Goncalves, U. Resende

Numerical Evaluation of Circuit Model for Fast Computational Analysis of Resonant Wireless Power Transfer System

F. M. Freitas[1], I. V. Soares[2], L. Krähenbühl[3], A. Bréard[3], C. Vollaire[3], S. T. M. Gonçalves[1], and U. C. Resende[1]
[1]Federal Center for Technological Education of Minas Gerais, DEE - PPGEL, 30421-169 Belo Horizonte, Brazil
[2]Institut d'Electronique et des Technologies du Numérique, IETR CNRS UMR 6164, 35700 Rennes, France
[3] Universite de Lyon, Insa Lyon, Université Lyon 1, Ecole Centrale Lyon, Ampère CNRS, 69134 Ecully, France

This paper proposes a circuit model to calculate the current along printed coils used in Resonant Wireless Power Transfer. It considers a system composed of a metamaterial and two coplanar coils, transmitter and receiver, respectively. First, a circuit model for the system is presented. Then, an analytical model is proposed to calculate the self-inductance of printed inductors, their characteristic resistance, and the mutual inductance between coils. The proposed formulation for calculating the mutual inductance between inductors is based on Neumann's formula. The practical results validate the model precision, obtaining a maximum deviation of approximately 8%, 3%, and 3%, respectively. Due to the generality of this approach, it can also be applied to more complex structures such as metasurfaces. The proposed 3-D models proved to be ideal for modeling the printed inductor. Furthermore, this model proved to be computationally more efficient for analyzing large systems when compared to commercial full-wave simulation software, with a reduction in the computational time larger than three orders of magnitude.

***Index Terms*—Circuit model, LC metamaterial, magnetic metamaterial, near field coupling, resonance, wireless power transfer.**

I. Introduction

RESONANT Wireless Power Transmission System (RWPT) is one of the inductively coupled wireless power transmission techniques. There are several approaches in which metamaterials are used between the wireless power link to increase transmission efficiency or focus the magnetic field [1].

Metamaterial-based RWPT systems are composed of multiple coils, which makes the computational simulation and optimization of these devices time-consuming, even in high-performance computers. Furthermore, in many RWPT projects, full-wave simulations are carried out in commercial software, which requires a highly dense mesh to obtain accurate results in analyzing complex structures. In addition, part of the design, such as the power and matching circuit, is developed in SPICE simulation environments. Therefore, this work aims to model RWPT systems to optimize design time and increase analysis capacity in the same interface.

The present paper proposes a semi-analytical approach for analyzing RWPT systems composed of printed transmitter and receiver coils interfaced by a metamaterial slab. This proposed model represents the system by a magnetically coupled circuit that calculates the current along the printed coils used in RWPT and the direct transmission coefficient. There are some formulations in the literature for calculating circuit parameters of complex resonant systems using Metasurfaces (MTS) [2], and efficiency analysis of symmetrical RWPT systems [3]. Nonetheless, the method for calculating the mutual inductance of wireless power transfer systems proposed in this work has the advantage of considering a 3-D approach in space and, to the author's best knowledge, is also the fastest.

Manuscript received November 2, 2022; revised December 16, 2022. Corresponding author: F. M. Freitas (email: felipe.machado@ieee.org).

II. Numerical Formulation

A. Topology of the RWPT Coils and the Metasurface

The RWPT system considered in this study is composed of two identical coplanar coils, transmitter (Tx) and receiver (Rx), positioned over a metamaterial slab with $N \times N$ unit cells, as shown in 1. In this work, the Tx and Rx coil and the metamaterial cells are geometrically identical. The square topology was chosen for the coils and unit cells since it has a higher quality (Q) factor than other geometries [4]. Additionally, the number of coil turns was chosen to achieve maximum self-inductance while maintaining a low characteristic resistance and ensuring a negligible parasitic capacitance between turns. Besides, a lumped capacitor is added to the metamaterial cells to tune its resonant frequency. Finally, the proposed topology is constructively simple, which allows us to prototype it through a copper etching process.

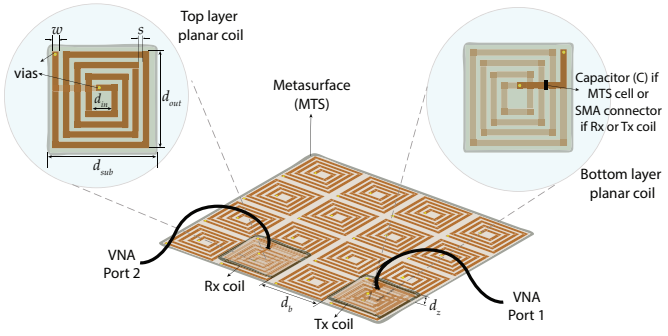

Fig. 1. Analyzed RWPT system and experimental setup. Square printed coil dimensions: number of turns (n) = 4, $d_{sub} = 50$ mm, $d_{out} = 46$ mm, $d_{in} = 10$ mm, $w = 3$ mm, $s = 2$ mm. The Tx and Rx loops are separated by $d_b = 50$ mm, and both are axially elevated at $d_z = 20$ mm to the metamaterial plane.

B. Circuit Model

The system shown in Fig. 1 can be modeled using the circuit shown in Fig. 2. The input power that feeds the Tx coil is generated by a known voltage source V_s with impedance Z_s. Then, the power is transferred to the metamaterial, which transmits to the Rx coil and then delivers to the load Z_L. Each coil can be represented as a series electric circuit that comprises an inductance L which represents its self-inductance, and resistance r which models the coil's characteristic resistance. In addition, for the metamaterial cells, a capacitance C is also included to account for the contribution of the lumped capacitor responsible for tuning the resonant frequency.

The magnetic coupling between the inductors that compose the system is modeled by the mutual inductance between each pair of coils. In Fig. 2, the mutual inductance between the Tx coil and each unit cell is represented by the arrow M_s, while M_r is the mutual inductance between the Rx coil and the unit cells. Besides, the mutual inductance between loops Tx and Rx is indicated as M_{sr}.

This circuit model (CM) can be analyzed as a linear system $Z_{(N+2)\times(N+2)} \cdot I_{(N+2)\times 1} = V_{(N+2)\times 1}$, where I is the unknown current matrix, V is the voltage matrix, and Z is the impedance matrix. The main diagonal of the Z matrix contains the self-impedance of each given coil, the capacitor present in the metamaterial cells, and the source resistance and load present in the Tx and Rx loops, respectively. In contrast, the other elements are the reactance due to all mutual inductance. Note that the symmetric nature of the Z matrix can be exploited to reduce the computational cost and speed up the numerical analysis.

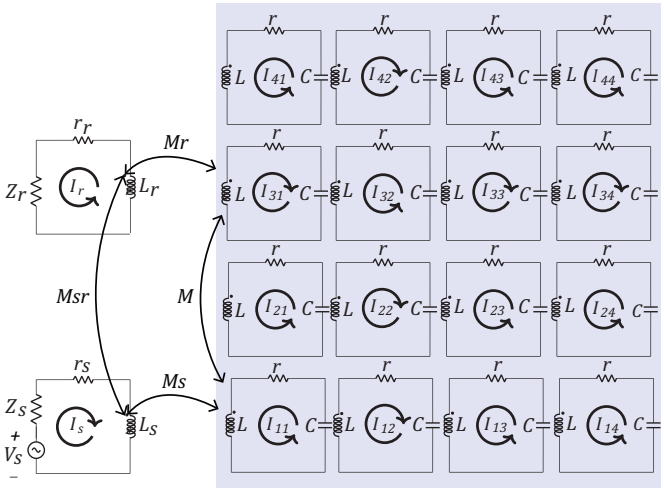

Fig. 2. Equivalent circuit for the two-coil system with resonant surface structure.

C. Calculation of the Characteristic Parameters of the Coil

This work applies the formulation presented in [5] to calculate the self-inductance of a printed inductor, in which the coil's inductance is given by:

$$L = \frac{K_1 \mu_0^2 n^2 d_{avg}}{1 + K_2 \rho_L} \tag{1}$$

where μ_0 is the magnetic permeability of the vacuum, $d_{avg} = 0.5 \cdot (d_{in} + d_{out})$, n is number of turns, and $\rho_L = (d_{in} - d_{out})/(d_{in} + d_{out})$. Finally, $K_1 = 2.34$ and $K_2 = 2.75$ are layout coefficients defined in [5]. Although (1) is an approximation for the self-inductance, it is proved to be computationally efficient, leading to values close to those measured as in [5].

The characteristic resistance of the printed coil (r) is composed by a static (DC) (r_{DC}) and a frequency-dependent (AC) component (r_{AC}) [6], that is:

$$r = r_{DC} + r_{AC} = \frac{\rho_r l}{A} + 320 \frac{\pi^4 d_{out}^4}{\lambda^4}, \tag{2}$$

where λ is the wavelength, l is the perimeter of the coil, A is the conductor cross-section, and ρ_r the resistivity of the conductor.

D. Calculation of the Mutual Inductance Between Coils

Generally, the mutual inductance is given by applying the Neumann's formula:

$$M_{sr} = \frac{\mu_0}{4\pi} \oint_{\Gamma_1} \oint_{\Gamma_2} \frac{\mathrm{d}\vec{r_i} \cdot \mathrm{d}\vec{r_j}}{r_{ij}}, \tag{3}$$

where Γ_1 and Γ_2 are closed paths in which flow the differential currents $\mathrm{d}\vec{r_i}$ and $\mathrm{d}\vec{r_j}$ defined in the tridimensional space $\mathbb{R}^3$, respectively, at a distance r_{ij} from the origin. Therefore, any arbitrary positioning between the coils can be evaluated through (3) by properly assigning the vectors $\vec{r_i}$ and $\vec{r_j}$.

In order to calculate the mutual inductance, consider the coplanar and parallel coils shown in Fig. 3(a) and Fig. 3(b), respectively. The parameters m_1, m_1', m_2, m_2' and h are shown in Fig.3 and the integration path must be closed as indicated by the dashed white line. The coil extremity highlighted in Fig. 3 can be excluded from the integration since the current density in this border part can be neglected. Apart from that, the microstrip lines presented in Fig. 3 are modelled as thin-wire structures located in the middle of the printed coil trace, which is a valid approximation in the operating frequency of RWPT systems once the trace thickness is much smaller than the wavelength and the geometrical size of the full structure [7].

The analyzed system presents symmetries that simplify the integral evaluation. First, the upper m_1 and lower m_1' limits of integration can be determined for each coil segment according to its point located in the xy plane. Consider y components for the odd segments and x for the even ones. In Fig. 3(a), for segment 3 of the left loop, $m_{1y} = d_{out} - w = a$ and $m_{1y}' = m_1 + a$ while the values of m_2 and m_2' can be obtained from the values of m_1 and m_1' referring to segment 1 of the reference loop. For instance, in the odd segments $m_{2y} = m_{1y} + dy$ and $m_{2y}' = m_{1y}' + dy$, where $dy = (a + e) \cdot dify$ in which a is the length of the longest segment, e is the distance between two vertical segments, and $dify$ the differential distance in y of the two coils. Conversely, for the even segments, $m_{2x} = m_{1x} + dx$ and $m_{2x}' = m_{1x}' + dx$, where $dx = (a+e) \cdot difx$ in which a is the length of the longest segment, e is the distance between two between horizontal segments, and $difx$ the differential distance in x of the two coils.

Finally, the value of h for each pair of segments corresponds to the distance between them. Therefore, for a pair of segments

segments i and j in Fig. 3, $h = dy + m_{2y} - m_{1y}$ if they are even, and $h = dx + m_{2x} - m_{1x}$ if they are odd. In this way, the integral that relates segment 3 of the first coil ($y_{1,3}$) and segment 1 of the second ($y_{2,1}$) can be written as:

$$M_{3,1} = \frac{\mu_0}{4\pi} \int_{m_{2y}}^{m'_{2y}} \int_{m_{1y}}^{m'_{1y}} \frac{\mathrm{d}\vec{y_{1,3}} \cdot \mathrm{d}\vec{y_{2,1}}}{\sqrt{h^2 + (y_{1,3} - y_{2,1})^2}}. \quad (4)$$

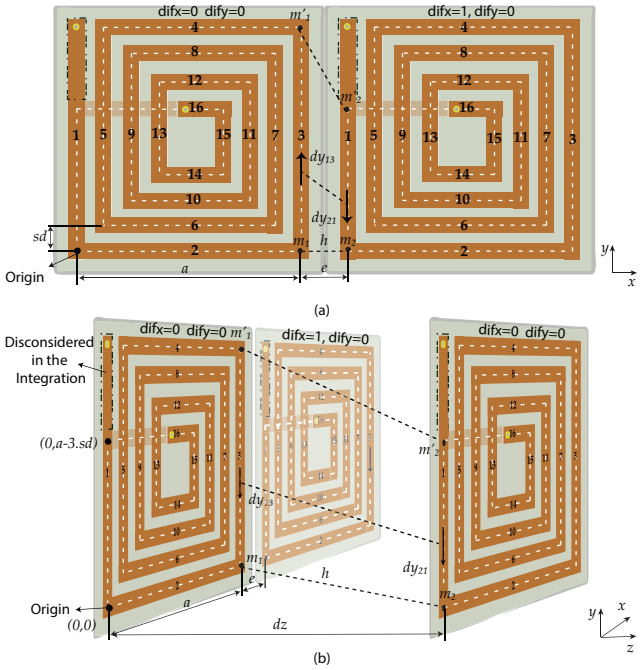

Fig. 3. Integration model contribution of segment 3 of the first coil ($y_{1,3}$) with segment 1 of the second coil ($y_{2,1}$) for the case: (a) two side by side coplanar coils; (b) two non-coplanar coils.

For the non-coplanar case, as shown in Fig. 3(b), the calculations of m_1, m'_1, m_2, and m'_2 are the same as in the coplanar case. However, for the calculation of h, we use $h = \sqrt{(dy + m_{1y} - m_{2y})^2 + dz^2}$ is used if they are even, and $h = \sqrt{(dx + m_{1x} - m_{2x})^2 + dz^2}$ if they are odd. The z-index indicates that the coil is axially separated from the other loop taken as a reference in the space. Finally, the distance between the segments is given by dz.

In (4) the contribution of a pair of coil segments is presented. Thus, to calculate the total mutual inductance, it is necessary to repeat this process for each pair of segments that composes the inductor geometry. Therefore, the number of iterations to calculate the mutual inductance between two coils is equal to $(N_{seg1} \cdot N_{seg2})/2$, where N_{seg1} is the number of segments of one loop and N_{seg2} of the other. However, perpendicular components have zero inductance, as in the pairs composed of odd and even segments. In this way, the number of iterations for evaluating the mutual inductance can be reduced by calculating only the contribution between the pairs of odd-odd M_{odd} and even-even segments M_{even}. Then, the total mutual inductance is given by the sum of these contributions, i.e., $M_{Total} = \sum_n M_{odd} + \sum_n M_{even}$.

Finally, the integral (4) can be solved using traditional numerical methods or by algebraic approximations such as proposed in [8]. In this work, the algorithm to calculate the mutual inductance was implemented in Matlab®. This script calculates the mutual inductance between the metamaterial unit cells using the coplanar case, whereas the mutual inductance between the receiver or transmitter coils and the unit cells corresponds to the non-coplanar analysis. In this case, as shown in Fig. 3(b), one of the coils (receiver or transmitter) is positioned at a specific axial separation from the resonant surface.

III. Experimental Validation

A. Measurement of the Characteristic Parameters of the Coil

In order to validate the numerical formulation in (1) and (2), the coil's inductance and resistance were measured using an impedance meter configured at a frequency of 24 MHz. This frequency was chosen due to the resonant frequency of the MTS. However, it was not verified significant variations in the operating range (1 to 30 MHz).

The comparison between the coil parameters calculated using (1) and (2) (CV) with those measured (MV) is shown in Table I. The deviation, calculated as $(CV - MV)/MV \times 100$, for the self-impedance was approximately 8%, which is a reasonable value compared to other methods and to the tolerance of commercial coils that can reach up to 20%. However, an 8% correction on the calculated value was taken into account in order to reduce the error propagation when simulating the full RWPT system. Conversely, for the characteristic resistance, a lower deviation of less than 3% was observed, which validated the proposed model.

TABLE I
Calculated and Measured Coil Parameters

	Calculated	Measured	Deviation
Self-Inductance	475 nH	437 nH	8.7%
Characteristic Resistance	76 mΩ	78 mΩ	2.6%

B. Evaluation of the Mutual Inductance Between Coils

First, the geometric approximation for the coil presented in Fig. 3 needs to be justified. For this, a full-wave simulation using the software CST® was carried out, and the surface current distribution in the printed coils at $24\,MHz$ is shown in Fig. 4. It is possible to verify that the current magnitude is higher in the internal region of the coil, whereas in the extremity, it significantly decreases, which justifies the proposed approximation.

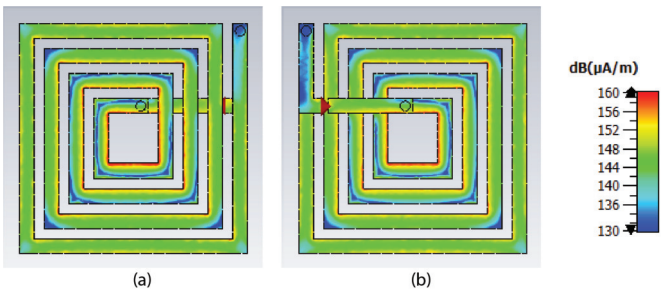

Fig. 4. Surface current distribution in the coil: (a) front view, (b) back view.

In order to validate the numerical model for the mutual inductance, three scenarios are considered. First, the side-by-side case with a 10 mm spacing between the coils, modeling the coupling M between the unit cells. Then, the mutual inductance M_{sr} between non-adjacent coplanar coils is evaluated by

the side-by-side case with 50 mm separation. Finally, the face-to-face scenario with 20 mm spacing represents the coupling between the Tx or Rx and the unit cell coaxially parallel to them, M_s and M_r, respectively. The comparison between the mutual inductance calculated for each case using (4) and the respective measurements performed on a Vector Network Analyzer (VNA) is shown in Table II.

TABLE II
CALCULATED AND MEASURED MUTUAL INDUCTANCES

	Calculated	Measured	Deviation
Side-by-side (gap 10 mm)	14.078 nH	14.295 nH	1.52 %
Side-by-side (gap 50 mm)	1.770 nH	1.784 nH	0.8%
Face-to-face (gap 20 mm)	81.256 nH	83.911 nH	3.16%

The results presented in Table II certify the model validation since the difference between the values obtained is very small and demonstrates its applicability for different coil arrangements and positioning. The difference may be due to measurement errors and some parameters not considered as the connector effects and parasitic capacitances. The mutual inductance for the presented cases was evaluated with the VNA also in the frequency of 24 MHz.

C. Frequency Analysis of RWPT Systems with MTS

The performance of the RWPT system is evaluated in terms of its transmission coefficient S_{21} between Tx and Rx coils, measured with the setup in Fig. 1. Moreover, the measured results are compared with those obtained with the proposed circuit model and simulations using a frequency solver and adaptive mesh refinement in CST®, as presented in Fig. 5. As can be noticed, both results are in good agreement for lower frequencies. However, the deviation increases with frequency once parasitic capacitances between coils and the losses in the substrate are disregarded in the CM but are taken into account in the full-wave simulation. Regarding the computational time, the electromagnetic simulation took about 609 s. In comparison, CM solved in 0.33 s, i.e., almost 1800 times faster, on a computer with an Intel® Xeon™ $W-2275$ processor, 256 GB RAM, and 3.30 GHz clock.

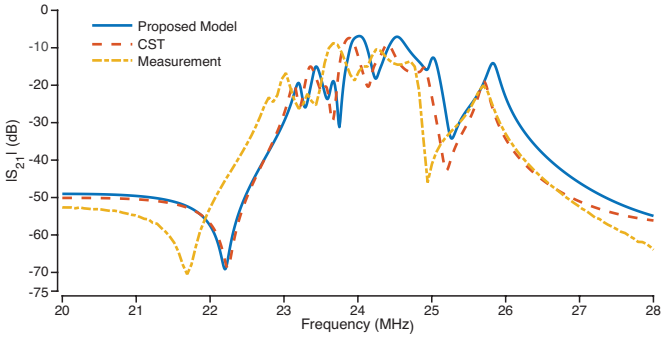

Fig. 5. Comparison between the transmission coefficient S_{21} calculated with the proposed approach, simulated in CST, and measured.

In Fig. 5, the system oscillation in frequency ranges from 22.3 to 28 MHz. Based on the calculated circuit parameters presented and validated, the value of the self-inductance used was 437 nH and the capacitance of 100 pF, leading to a resonant frequency around 24 MHz. Therefore, as indicated in Fig. 5, the optimal frequency, that is, the frequency in which the efficiency reaches its maximum, is precisely the resonant frequency of the MTS.

Compared to measurements, a frequency deviation of approximately 300 kHz on the $|S_{21}|$ values was observed in Fig. 5. This deviation is mainly due to the tolerance of the lumped capacitors of the MTS cell. Even though the system was prototyped with capacitors with a 1% tolerance capacitor, this slight variation is enough to shift the optimal frequency once resonant WPT systems are significantly narrowband. Another difference in the measurement curve is that the MTS operating band is slightly larger and has a more accentuated decay at higher frequencies. It is caused by the Equivalent Series Resistance (ESR) of the physical capacitors that lead to a slight reduction in the quality factor. Besides, electromagnetic interferences and the connector influence also are not considered in simulations and may affect the measured values.

IV. CONCLUSION

This paper proposes a circuit model to reduce the computational cost of analyzing complete RWPT systems. First, the circuit model of an RWPT system was elaborated. Then the 3-D mathematical formulation based on circuit theory, which is necessary for calculating currents in the coils, is presented. Subsequently, mathematical expressions were proposed to calculate the circuit parameters of the RWPT system, such as the self-inductance and characteristic resistance of the coils. Subsequently, the algorithm for calculating the mutual inductance between the loops was described. Finally, the validation and frequency analysis were carried out.

The results showed that the proposed approach reproduces the behavior of the system, allowing us to find numerical values of S21 very close to those found through electromagnetic simulations in commercial software, with a reduction in the computational time larger than three orders of magnitude. Finally, this formulation can be extended to synthesize more complex RWPT-based devices and ensure computational savings in their design.

ACKNOWLEDGMENT

This work was partially supported by FAPEMIG, CAPES, CNPq, CEFET-MG and Laboratoire Ampère - CNRS UMR 5005.

REFERENCES

[1] I. Soares and U. Resende, “Radially periodic metasurface lenses for magnetic field collimation in resonant wireless power transfer applications,” *J. Microw. Optoelectron. Electromagn. Appl.*, vol. 21, pp. 48–60, 2022.
[2] L. Krähenbühl *et al.*, “Large surface LC-resonant metamaterials: From circuit model to modal theory and efficient numerical methods,” *IEEE Trans. Magn.*, vol. 56, pp. 1–4, 2020.
[3] Zeng, Y.*et al.*, ”Analysis and design of asymmetric mid-range wireless power transfer system with metamaterials”. *Energies*, vol. 14, pp. 1348, 2021.
[4] Mao, Shitong *et al.*, ”A polygonal double-layer coil design for high-efficiency wireless power transfer”. *AIP Advances*, v. 8, n. 5, p. 056631, 2018.
[5] S. Nishimura *et al.*, “Enhancing the inductive coupling and efficiency of wireless power transmission system by using metamaterials,” in *Proc. Brazilian Symposium of Microwave and Optoelectronics*, pp. 121–125, 2014.
[6] D. Hui, Z. Yisheng, and Z. Baishan, “Research on the electromagnetic radiation of a PCB planar inductor,” in *Proc. 2005 Asia-Pacific Microwave Conference Proceedings*, vol. 1, pp. 3, 2005.
[7] C. A. Balanis, *Antenna theory: analysis and design*. John Wiley & Sons, 2015.
[8] E. Durand, *Magnétostatique*. Elsevier Masson, pp. 178, 1968.